20 August 1971, Volume 173, Number 3998 SCIENCE

Preliminary Examination of Lunar Samples from Apollo 14

A physical, chemical, mineralogical, and biological analysis of 43 kilograms of lunar rocks and fines.

The Lunar Sample Preliminary Examination Team (*1*)

The surface of the moon can be divided into the dark mare areas and the bright highland regions. The mare regions cover about one-third of the near side of the moon and make up a small fraction of the far side. These mare areas are recognized as the areas of most recent widespread rock formation on the lunar surface. The first three groups of samples returned from the moon to earth, that is, the samples from the Apollo 11, Apollo 12, and Luna 16 missions, all come from typical mare regions.

Detailed chemical and petrographic studies of the samples from the three widely separated mare regions show that the dark regions of the moon are probably underlain by basaltic rocks that are iron-rich and sodium-poor (relative to similar terrestrial rocks). Absolute ages determined for basaltic rocks from the Apollo 11 and Apollo 12 sites and crater densities on nearby mare surfaces suggest that the final filling of most mare basins took place between 3.0×10^9 and 4.0×10^9 years ago.

The stratigraphic and petrographic studies of the mare samples lead to two general inferences regarding the moon: (i) that the internal temperatures of at least parts of the moon reached the melting point of basalt less than 1×10^9 years after the formation of the moon, and (ii) that the evolution of most of the surface of the moon took place very early in its history. Gilbert (*2*) and several other authors have suggested that one of the last major events in the evolution of the premare lunar surface was the formation of the Mare Imbrium basin along with an extensive blanket of material that was ejected from this basin by the Imbrian impact. This blanket was named the Fra Mauro Formation after a region north of the crater Fra Mauro where a portion of the presumed ejecta blanket appears to protrude above the surrounding mare basalt flows (*3*). On 5 and 6 February 1971 the Apollo 14 lunar landing mission visited a site approximately in the center of this island of premare material.

Astronauts Shepard and Mitchell landed at a site (3°40′19″ south, 17°27′46″ west) 1230 kilometers south of the center of the Imbrium basin on 5 February 1971. About 43 kilograms of rock and soil samples were returned from points on traverses that spanned a distance more than 1 kilometer long. Further details on the regional and local geology are given in an accompanying report (*4*). The total collection includes 33 rocks that weigh more than 50 grams each and about 30 smaller rocks that weigh from 10 to 50 grams each. Four core tubes of soil were collected, two of which were driven end to end as a double core tube. The "Apollo 14 Preliminary Science Report" (*5*) lists details on the mass and location of individual samples.

The preliminary examination of these rocks began on 11 February. This study included biological, mineralogical, chemical, and isotopic measurements that were intended (i) to provide data necessary for the division and distribution of these samples for thorough and detailed investigations, and (ii) to determine whether or not these samples posed a threat to the terrestrial biosphere. Techniques used were in general the same as those for previous missions (*6*) with the exception that no analyses for organic compounds were performed. Rocks ranging from about 1 gram to the largest rock returned were characterized by means of low-power binocular microscopes. Limited portions of selected rocks were sampled for chemical analysis and thin-section preparation, and these small samples may not be representative of the whole rock.

All samples were processed in pure nitrogen [less than 10 parts per million (ppm) of contaminant gases] in stainless steel glove cabinets designed to provide biological containment. Contaminant concentrations of the gases hydrogen, oxygen, carbon monoxide, carbon dioxide, methane, and argon were monitored by gas chromatography and oxygen and water vapor monitors. In order to establish base levels for particulate contaminants in the cabinets, monitors were exposed prior to the processing of samples.

All of the samples photographed and collected on the Apollo 14 mission were probably transported by relatively recent impacts on the lunar surface. The majority of the samples are probably associated with the formation of Cone Crater. The access to this very fresh crater provided an opportunity to examine a large number of rocks with a wide range of sizes. There is an abundance of rocks in the vicinity of this crater.

A second small boulder field, which was probably originated from Cone Crater, was seen immediately north of the landing area during the first extra-

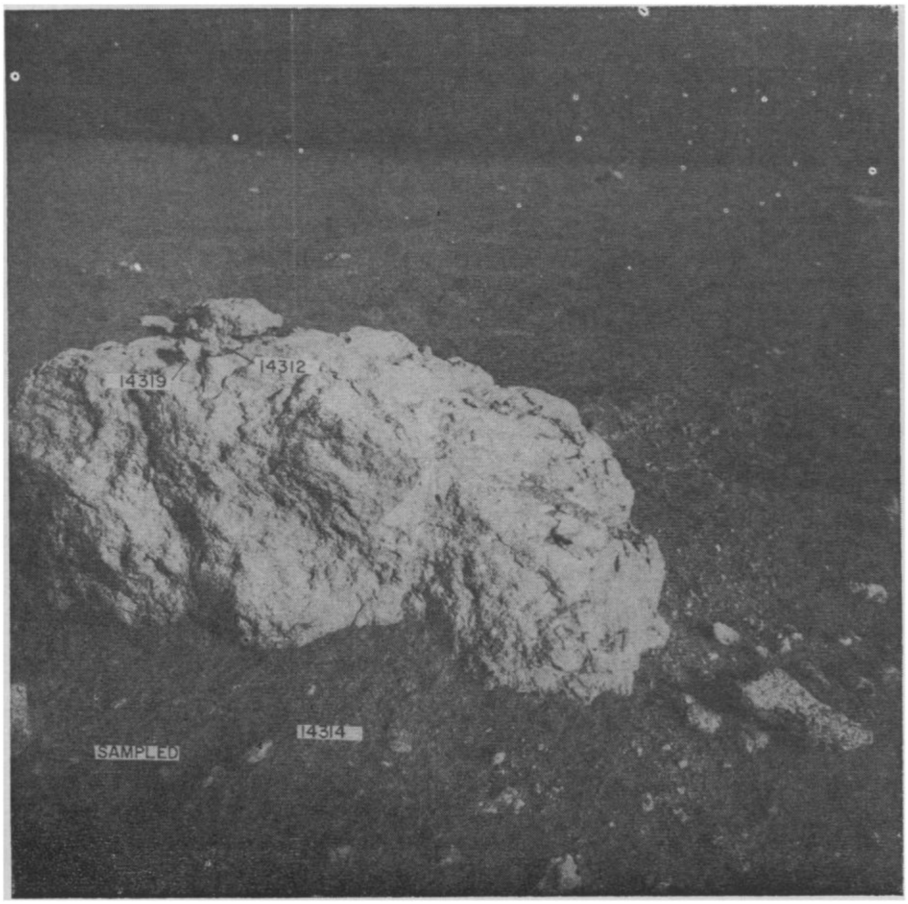

Fig. 1. One of the large boulders in the northwest boulder field (northwest of the lunar module). Rocks that were collected by the astronauts are identified. White clasts are visible in the boulder.

vehicular activity (EVA 1). The largest boulder in this area was photographed by astronaut Mitchell during EVA 2. One of these photographs (Fig. 1) shows the portion of the rock that was sampled. An even larger rock was sampled at the edge of Cone Crater. The returned sample, along with its parent rock, is shown in Fig. 2. The lunar surface photographs of both of the large rocks (Figs. 1 and 2) clearly show that these rocks are heterogeneous on a scale of tens of centimeters. The rock shown in Fig. 1 includes a white angular inclusion with remarkably sharp boundaries. The white rocks shown in Fig. 2 contain several rounded, very dark inclusions.

Macroscopic examination of the returned specimens indicates that the heterogeneities observed on the lunar surface extend to much smaller scaled features within the returned rocks. A variety of clasts or inclusions set in a matrix of fine-grained material is found in almost all the Apollo 14 specimens. The complex lithologic textures seen in these rocks clearly indicate that the sequence of events that led to their formation must be rather extensive; that is, their origin cannot be described in terms of a single event. These macroscopic heterogeneities are well illustrated in sample 14321 (Fig. 3). Indeed, only two out of the 35 large samples that were returned appear homogeneous on the scale observed by the naked eye. Both of these rocks are typical phaneritic igneous rocks. The large-scale heterogeneity observed on the lunar surface suggests that it is possible that even these two homogeneous rocks could have been clasts in larger rocks. The Apollo 14 rocks are potentially much richer sources of information on lunar history than the simple igneous rocks returned from earlier lunar landings.

Texture and Mineralogy

The textural diversity of the Apollo 14 rocks is probably the most fundamental and significant characteristic of these rocks observed during the preliminary examination. Some of the Apollo 14 rocks are, indeed, similar to the breccias from the Apollo 11 site, but the range of textural characteristics is much greater than that observed in earlier lunar samples. In general, the fragmental rocks consist of a variety of rocks and mineral clasts set in matrices which range from a friable fine-grained, clastic mass to a fine-grained, very coherent mosaic of interlocking crystals. Relative to the breccias returned by the Apollo 11 and Apollo 12 missions, some of the Apollo 14 rocks are lighter in color, more friable, and contain fewer and smaller clasts, but the majority are more coherent, contain less glass, and have larger and more abundant clasts. Matrices range from those with exclusively clastic textures (such a matrix discussed below is termed one with a low degree of crystallinity) to those that contain euhedral to subhedral crystals and whose textures resemble those of some metamorphic rocks (high degree of crystallinity). In rocks with an intermediate degree of crystallinity, some ilmenite and plagioclase grains commonly exhibit crystal faces.

We attempted to classify the fragmental rocks on the basis of the following criteria: (i) coherence, (ii) percentage of clasts larger than 1 millimeter in diameter, (iii) color of the lithic clasts, and (iv) degree of matrix crystallinity. A limited thin-section study suggests that the degree of crystallinity of the matrix will prove to be a significant parameter for classification when a more extensive microscopic survey of the classic rocks has been made.

A working classification was developed on the basis of a study of hand specimens. The fragmental rocks fall into three groups, each of which is represented by about one-third of the rocks.

Samples in group 1 are those that have friable matrices and contain about 5 percent clasts larger than 1 millimeter, among which lithic clasts predominate. In more than half of these rocks light-colored clasts make up more than 90 percent of the total clasts larger than 1 millimeter in diameter; the remainder have less than 50 percent dark-colored clasts. The majority of the clasts are themselves fragmental. Angular glass fragments and broken and intact glass spheres, which are mostly medium-brown in color, are present. A number of the samples bear the marks of the thin aluminum foil used to wrap and protect them and they crumble very easily. They resemble weakly indurated soil.

Samples in group 2 are characterized by a higher proportion of light-colored clasts than dark-colored clasts and by moderate coherency. The abundances of the clasts are high; nearly 80 percent of these rocks contain more than 5 percent clasts larger than 1 millimeter in diameter, and many rocks contain considerably more than 5 percent clasts. In about 60 percent of these rocks, leucocratic clasts make up more than 90 percent of the total lithic clasts. There are some clasts of basaltic rock, some of a very fine-grained melanocratic rock, and a few monomineralic granular olivine clasts.

Samples in group 3 are characterized by a larger proportion of dark-colored lithic clasts than light-colored clasts. Ninety percent of the rocks in this group contain 5 percent or more clasts larger than 1 millimeter in diameter. The majority of the clasts are crystalline, aphanitic, dark gray to black fragments, with recrystallized matrices. Basalt and "dunite" clasts are present in some rocks.

Rounded clasts are common, although angular clasts predominate (Fig. 3). Lithic clasts range in size from a few micrometers to 16 centimeters (sample 14321). Lithic clasts can be classified as fragmental clasts (fragments which themselves are composed of fragmental material) and homogeneous, largely crystalline clasts. Fragmental clasts are generally more abundant than homogeneous crystalline clasts. Most fragmental clasts contain the same range of clast types as the host rock and are distinguishable only by virtue of differences in their matrices. The degrees of crystallinity of the clasts are equal to or greater than that of the matrix. Boundaries in clasts with matrices may range from sharp to diffuse; both types of boundaries may be found in the same rock. Up to three generations of fragmental rocks within clasts have been observed.

A short description of the nonfragmental lithic clasts in order of abundance follows.

1) Clinopyroxene-plagioclase clasts with basaltic texture are common and generally contain minor amounts of ilmenite, metallic iron, and troilite (Fig. 4). Plagioclase grains commonly show a fine mosaic; mosaicism in pyroxene is less abundant.

2) Feldspathic clasts which consist principally of plagioclase with only minor amounts of other phases [pyroxene, olivine(?), ilmenite, metallic iron, and zircon(?)] are fairly abundant. Plagioclase grains are commonly enclosed by a very fine-grained feldspathic matrix. Many plagioclase grains are deformed, and fine plagioclase mosaics are not uncommon. Some feldspar grains show no deformation and are composed of plagioclase with a granulitic texture (Fig. 5).

3) Plagioclase-orthopyroxene clasts with subophitic texture contain intergrown plagioclase and orthopyroxene

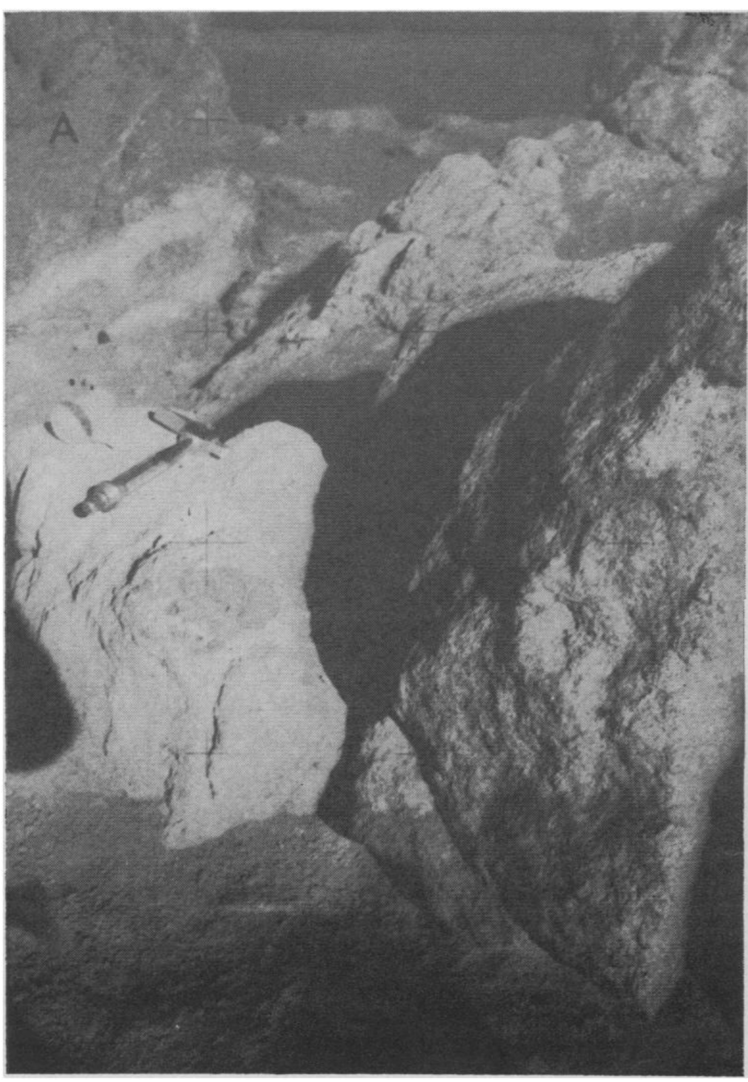

A

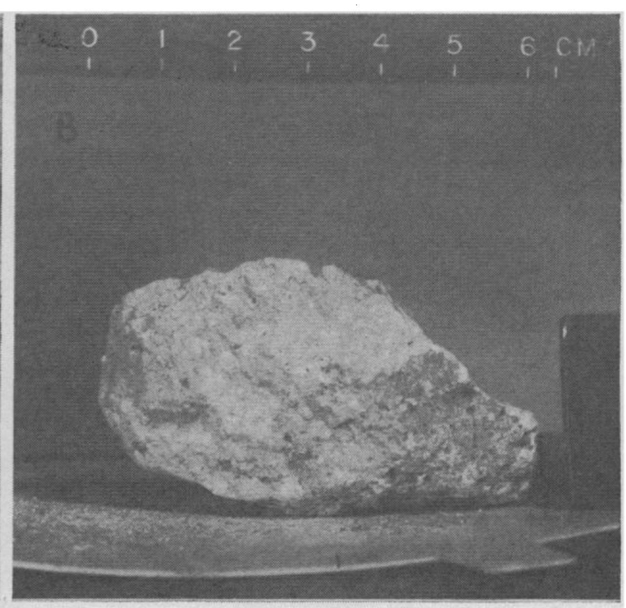

B

Fig. 2. (A) View of boulders near the rim of Cone Crater. The white rock (sample 14082) was chipped from the boulder in the foreground, just below the end of the hammer handle (41 centimeters long). Note the large, dark clasts in this boulder and other inhomogeneities in other boulders. (B) Rock 14082, a fragmental rock with a light-colored matrix. It contains few lithic clasts and many feldspar clasts.

with minor amounts of clinopyroxene, ilmenite, and iron. Euhedral plagioclase is accompanied by anhedral pyroxene, and in some cases the orthopyroxene is poikilitic.

4) Olivine-glass clasts are rare and consist of skeletal olivine crystals in glass.

5) Clasts consisting almost entirely of olivine with a granulitic texture are present in some rocks.

6) Angular glass clasts and glass spheres are present in those rocks that do not have a crystalline matrix. The glass ranges in color, amount, and type of inclusions and in heterogeneity. Some glass clasts are apparently devitrified, one type consisting of relic angular plagioclase and pyroxene grains in an extremely fine-grained groundmass containing skeletal olivine(?) microlites. All glass clasts in the recrystallized fragmental rocks are at least partially devitrified, containing needle-like crystals of feldspar(?).

Mineral clasts in the fragmental rocks that have been studied microscopically include anorthitic plagioclase, clinopyroxene (augite and pigeonite), orthopyroxene, ilmenite, olivine, iron metal, troilite, chrome spinel, ulvöspinel, native copper, armalcolite, zircon, apatite, potassium feldspar(?), and several unidentified phases. A pink, high-relief, isotropic mineral in several of the fragmental rocks may be garnet or spinel. The ratio of plagioclase to clinopyroxene ranges very roughly from 2 : 1 in many fragmental rocks to about 5 : 1 in some of the lighter-colored fragmental rocks. A brief description of the more abundant minerals follows.

Plagioclase occurs as single grains and commonly also as fine-grained mosaics probably produced by shock effects on single crystals. A few clasts consist of an equigranular mosaic of plagioclase crystals which differ from the above in being considerably more coarse-grained. Some maskelynite is present.

Clinopyroxene is abundant, with both pigeonite and augite represented. Some clinopyroxene grains are large and undeformed and contain fine, very regular exsolution lamellae of pyroxene, but deformation and mosaic texture are common. Orthopyroxene, which may contain lamellae of clinopyroxene up to 5 micrometers wide, is commonly undeformed.

Olivine occurs as angular single crystals; a few grains are subhedral. Some clasts up to 1 millimeter in diameter are an equigranular mosaic of olivine grains. Several olivine clasts are rimmed by an intergrowth of pyroxene and ilmenite.

Ilmenite is the most abundant opaque mineral, although it is less abundant than in earlier lunar samples. It commonly occurs as small angular to subrounded grains, and, in the fragmental rocks showing some degree of crystallinity, small (10-micrometer) laths occur. A few large (up to 250 micrometers) subrounded grains occur; many of these show deformation-twin lamellae.

Metallic iron is widely dispersed throughout the rocks and occurs in grains ranging from less than a micrometer to 250 micrometers in diameter. The grains range in shape from rounded to ragged and highly irregular. The abundance of metal is commonly less than that in Apollo 12 basaltic rocks. The association of metal with troilite is less pronounced than in the Apollo 11 and Apollo 12 rocks.

Troilite is less common in the Apollo 14 samples than in the Apollo 11 and Apollo 12 rocks and occurs as small rounded to angular grains which may contain inclusions of native iron. Chrome spinel, ulvöspinel, native copper, and armalcolite occur as angular grains in extremely minor amounts.

Most of the mineral clasts are such as might be expected from comminution of the lithic fragments. However, the sparsely occurring single mineral fragments of clinopyroxene and orthopyroxene with exsolution lamellae and of olivine and ilmenite in larger grains have not been seen in lithic clasts.

Matrices of fragmental rocks display a range of crystallinity. One extreme type contains abundant glass, and in these the fragments range in size to less than a micrometer. At the other extreme, some matrices appear to be totally crystalline; in these, the matrix consists of lath-shaped plagioclase, anhedral pyroxene, plate-like ilmenite, and small metal grains. The bulk of the matrices of fragmental rocks appears to exhibit some degree of crystallinity, and the examples with totally

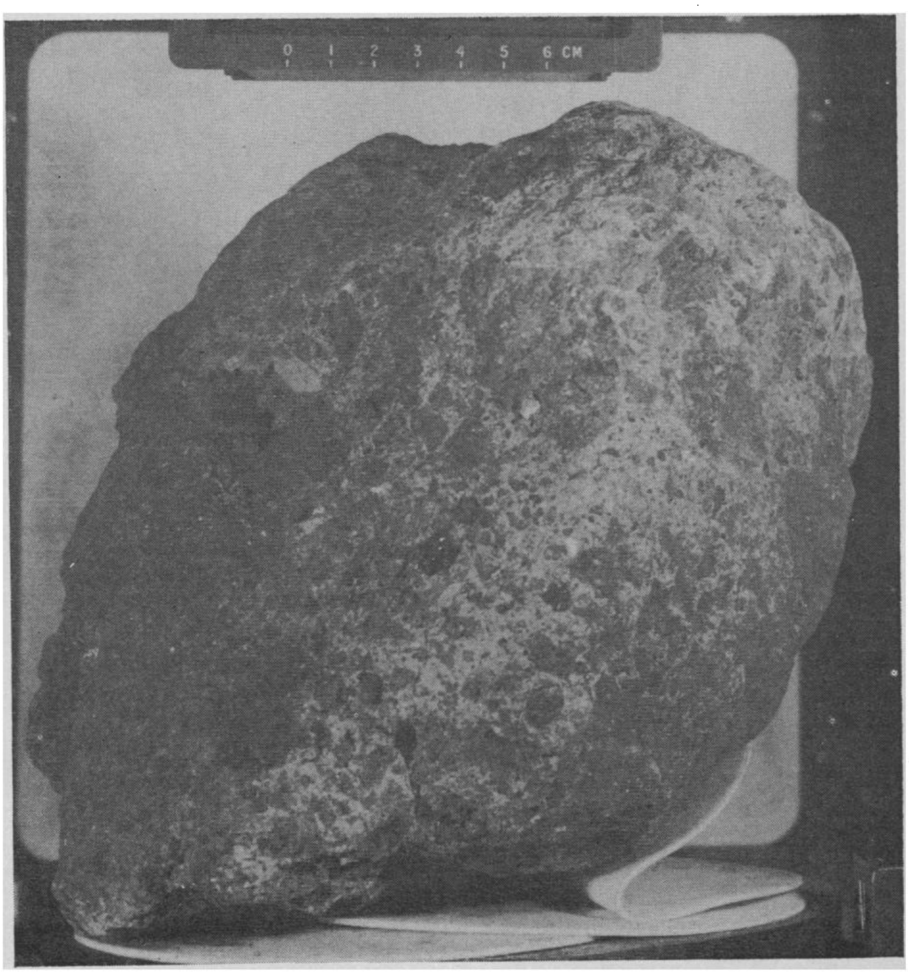

Fig. 3. Rock 14321 (the largest rock returned, 8.9 kilograms). This rock is fragmental with a medium-gray matrix and contains abundant dark fragmental clasts. One clast is 10 centimeters in diameter.

crystalline matrices would be classed as crystalline rocks of fragmental origin.

Some of the fragmental rocks studied in thin section contain dark-brown glass that occurs in two ways: (i) filling fractures and veins, up to 5 millimeters thick, which may crosscut matrix and clasts, and (ii) coating some clast surfaces. Most of the glass veins and coatings contain mineral inclusions and spherules of metallic iron, and some are vesicular. The rocks tend to break along glass-filled fractures.

Homogeneous Crystalline Rocks

The homogeneous crystalline rocks can be divided into two groups, those with basaltic textures and those with very fine-grained granulitic textures. The only crystalline rocks over 50 grams are samples 14053 and 14310. These two basaltic rocks are composed principally of plagioclase, brown and yellow-brown pyroxenes, olivine, and opaque minerals. These rocks differ from the basaltic rocks returned on the Apollo 11 and Apollo 12 missions in being much richer in plagioclase and poorer in ilmenite, and in having much lighter-colored pyroxenes.

The basaltic rocks are fine- and even-grained, are aphyric, and have textures ranging from intersertal to intergranular to ophitic. Grain size ranges from fine to medium and is commonly coarser than that of the homogeneous nonbasaltic crystalline rocks. The basaltic rocks fall readily into two subgroups, one having about 40 to 45 percent (by volume) plagioclase (samples 14053, 14071, and 14074) and the other having about 60 to 70 percent plagioclase (samples 14073, 14078, 14079, 14276, and 14310).

Rock 14310 is a fine-grained basaltic rock with scattered small cognate inclusions that are finer grained than the body of the rock (Fig. 6). Rock 14310 has an intergranular to intersertal texture and consists of euhedral plagioclase laths and anhedral pyroxene crystals. Modal analyses indicate that the rock contains about 66 percent plagioclase, 31 percent clinopyroxene, and lesser amounts of ilmenite, troilite, iron metal, chrome spinel, and ulvöspinel. The mesostasis, which amounts to a few volume percent, consists of complex fine-grained material, including apatite(?), ilmenite, troilite that contains blebs of metallic iron, possible alkali feldspar, an unidentified orange-brown, transparent, isotropic mineral with high relief and high index of refraction [tranquillityite(?)], and clear glass containing opaque to reddish-brown glass(?) spherules.

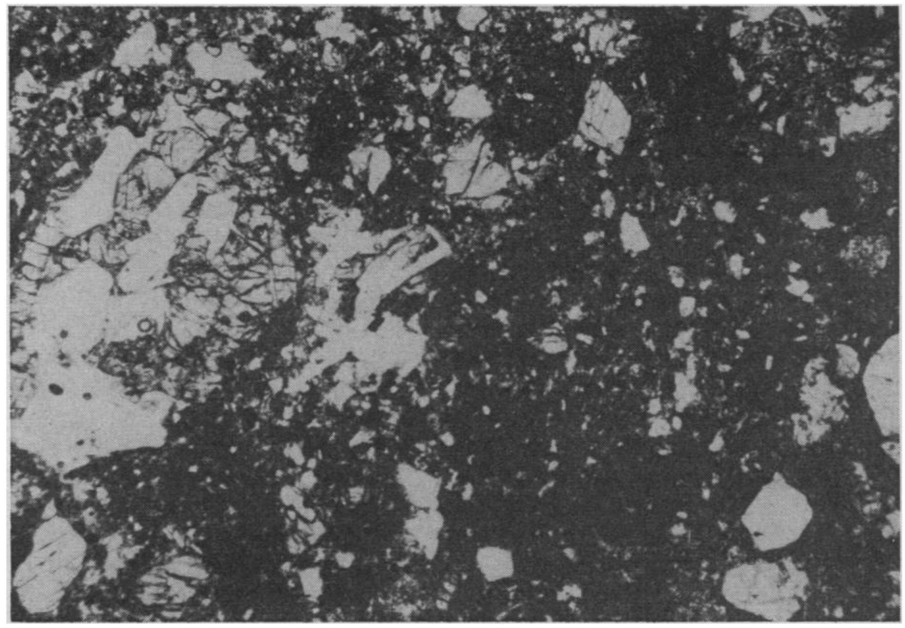

Fig. 4. Photomicrograph of a thin section of rock 14304 illustrating a fragmental rock containing a large clast with basaltic texture and many mineral and fragmental clasts. (Field width, 3.1 millimeters.)

Sample 14053 has an ophitic texture, and is more coarse-grained and richer in ferromagnesian minerals than sample 14310. The rock is moderately inhomogeneous and appears to be subtly layered, with about 40 percent modal plagioclase in one part and about 60 percent in the remainder. One thin section of this rock is composed of pyroxene (51 percent, mainly pigeonite), bytownitic or anorthitic plagioclase (41 percent), and a few percent olivine, which is commonly present as anhedral grains in cores of pigeonite grains. Phases in minor abundance include metallic iron, ilmenite, troilite, and ulvöspinel with ilmenite lamellae along

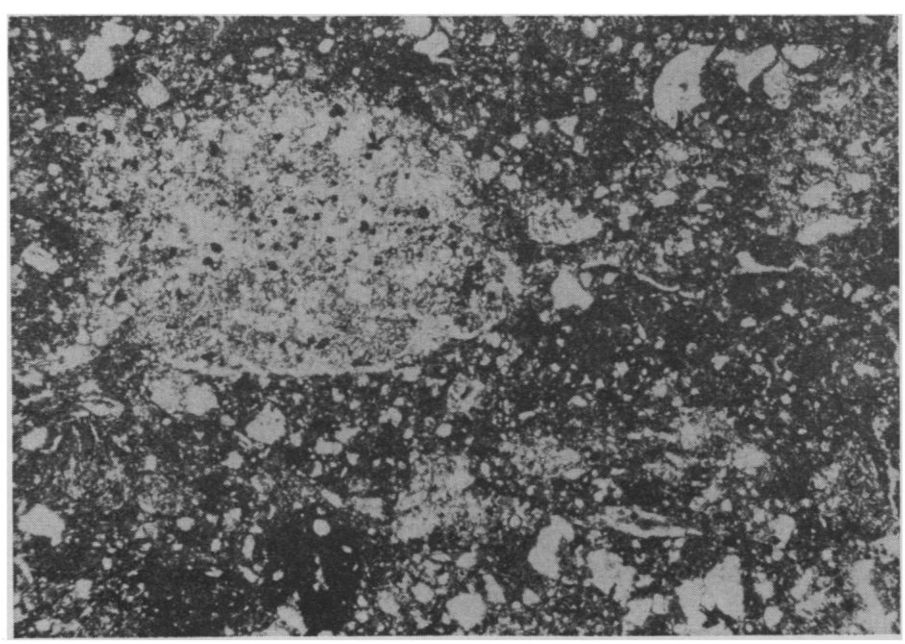

Fig. 5. Photomicrograph of a thin section of rock 14301 illustrating a fragmental rock containing abundant lithic clasts. The large clast is an example of the fine-grained granular feldspathic clasts. Other lithic clasts include a broken glass spherule and a dark matrix fragmental clast. (Field width, 3.1 millimeters.)

octahedral planes. Cristobalite (about 2 percent) occurs in vugs and is associated with the mesostasis. The mesostasis is complex and includes spongy masses of metallic iron, dendritic ilmenite, fayalite(?), and vermicular mixtures of colorless and black glasses.

The fine-grained holocrystalline rocks with granulitic texture contain 1 to 5 percent large mineral grains, commonly plagioclase, but less commonly olivine or pyroxene. Their fabric is commonly inequigranular. All but two rocks in this group are light colored and consist principally of plagioclase and light-gray pyroxene. The two dark rocks (samples 14006 and 14440) are aphanitic, and their mineralogies are not yet known since no thin sections were examined. Both the light and dark rock types appear to be common as clasts in the fragmental rocks. The lithologic similarity of these rocks to clasts and their small sizes support the idea that these rocks were once clasts in fragmental rocks.

Shock-Metamorphism

Shock features are best developed within individual clasts of fragmental rocks and in soil particles and are largely absent from basaltic rocks. Within fragmental rocks the evidence for shock decreases with the increasing crystallinity of the matrix. As in earlier lunar samples, there is abundant evidence of multiple shock events: as many as three "generations" of clasts within a fragmental rock may contain evidence of shock metamorphism.

Weak shock. Most lithic and mineral inclusions within the fragmental rocks are intensely fractured and shattered. Extreme mosaicism is common and is one of the most outstanding features in the fragmental rocks. No deformation structures unequivocally indicative of static deformation were observed, and it is therefore concluded that the abundant mosaicism is, to a large extent if not exclusively, due to weak shock effects below the Hugoniot elastic limit.

Moderate shock. Shock features indicative of solid-state deformation are present in fragmental rocks and soils. These include: planar features in plagioclase, pyroxene, and olivine associated with a decrease in refractive index; pressure twinning in plagioclase and pyroxene; and diaplectic feldspar glasses. Despite the high abundance of lithic and mineral clasts, however, these features are as rare as they were in the Apollo 11 and Apollo 12 materials.

Strong shock. Shock-fusion products are present as heterogeneous schlieren-rich glass fragments and glass spheres which in some cases contain mineral relics. Some lithic clasts contain veins of shock-melted glass containing numerous metallic spherules. In addition, glass spatter of various shapes and sizes was observed on the surfaces of some rocks. Thus, as in samples from earlier missions, there is widespread evidence for shock-induced fusion.

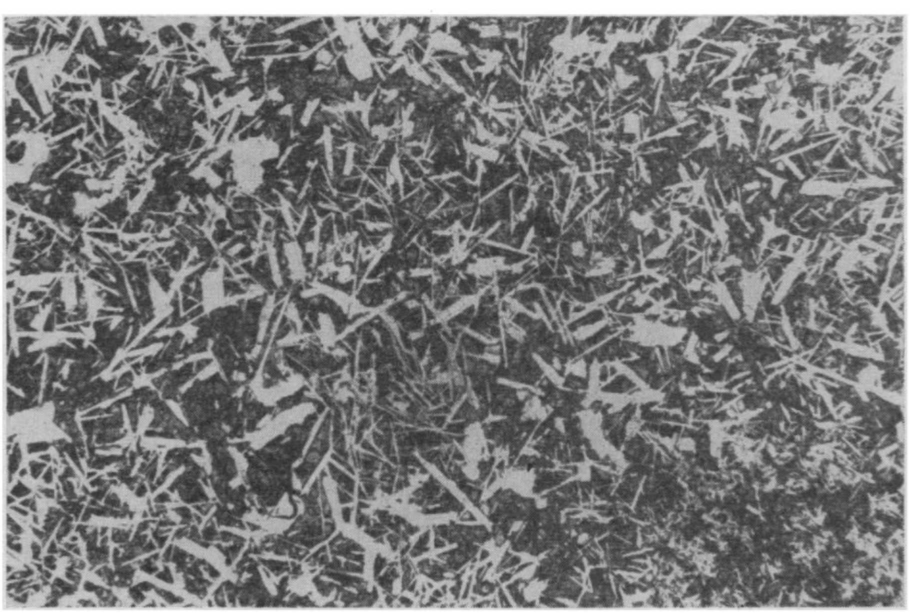

Fig. 6. Photomicrograph of a thin section of rock 14310 illustrating the intergranular texture of the plagioclase and pigeonite and showing a cognate inclusion in the lower right corner. (Field width, 3.1 millimeters.)

Rock Surface Features

In general, the surface features observed on Apollo 14 rocks are similar to those reported for earlier lunar samples (6). Micrometeoroid impact craters are very common and are characterized by a central glass-lined depression (pit) and a concentric area of conchoidal fractures (spall zone). Some exceptionally large pit craters, up to 5 millimeters in pit diameter, were observed. Some friable rocks have craters without glass-lined central pits and no pronounced spall zone; their shapes are typical for craters in slightly cohesive targets (7). The most friable rocks do not display any signs of cratering; such may have been destroyed in transit from the moon.

Melt droplets and small glass spatter of various shapes, sizes, and colors are common on rock surfaces. Large glass coatings (1 to 3 square centimeters) are rare. When present, they seem to be thinner and much more vesicular than spatter on rocks from earlier missions and range from about 0.1 to 1 millimeter in thickness. In addition, glass fills fractures in some rocks. In one case metallic spatter (a few square millimeters in size) was observed.

A few rocks display planar surfaces (10 to 50 square centimeters) that are characterized by parallel grooves a few millimeters apart and up to 1 millimeter deep. These surfaces otherwise are free of relief and resemble slickensides. A soil line separating a dust-covered "bottom" from a dust-free "top" surface was observed on some rocks. Less cohesive fragmental rocks with a high percentage of lithic inclusions have hackly surfaces characteristic of molds of clasts. In general, the surface features observed on the moderately cohesive and cohesive rocks are similar to those reported for earlier lunar samples.

Soil

Although the surface texture and appearance are similar to those at the Apollo 11 and Apollo 12 landing sites, there is a greater variability in the characteristics of the soil at depths of a few centimeters than had previously been encountered.

The walls of a trench which the astronauts dug collapsed at a depth of 33 centimeters, which is considerably shallower than the depth of 100 to 200 centimeters that had been predicted.

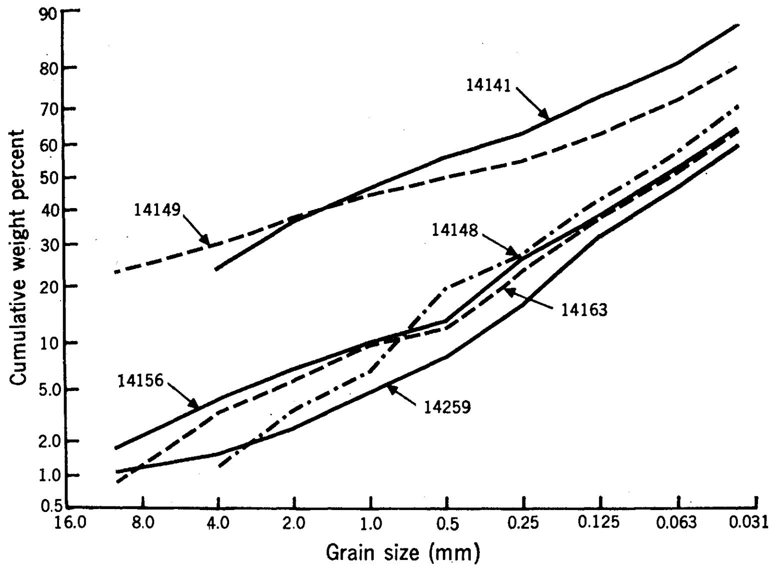

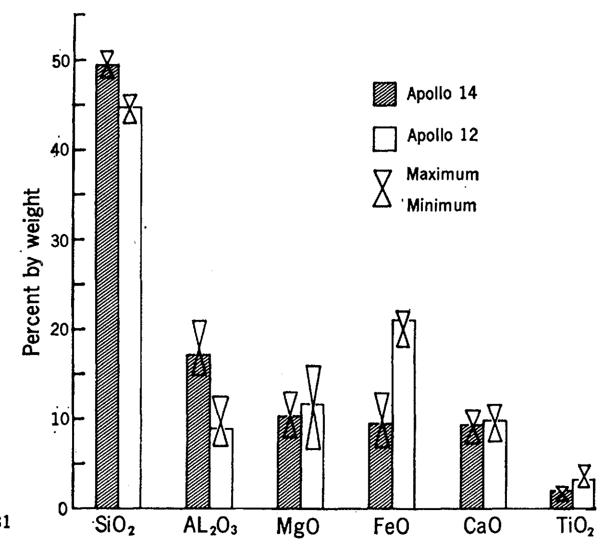

Fig. 7 (left). Size distributions of six Apollo 14 soil samples. Fig. 8 (right). Comparison of the contents of the major elements for Apollo 12 and Apollo 14 rocks. The top of the bar represents the mean composition.

Calculations indicate that the cohesion of the soil at the trench site may be as small as 10 percent of the values observed on earlier missions (3.5 to 7 kilonewtons per square meter).

Seven soil samples were returned by the Apollo 14 mission. Figure 7 shows the size distributions for six of these samples. Four samples (samples 14148, 14163, 14156, and 14259) have grain-size distributions similar to those of the Apollo 11 and Apollo 12 soils, except that they are more poorly sorted. Two samples (samples 14149 and 14141) are coarser than any lunar soil samples previously examined, with the exception of the coarse layer in the Apollo 12 double core (sample 12028).

The < 1-millimeter fractions of the more fine-grained soils are characterized by the following characteristics: (i) there is a high glass content; (ii) lithic fragments and a higher proportion of glass than mineral fragments are present in the coarser material of this fraction; the reverse conditions are the case in the smaller sizes; (iii) plagioclase and pyroxene are the most abundant minerals; and (iv) there is a range of values for the ratio of plagioclase to pyroxene.

Soil samples 14163, 14148, and 14149 contain 40 to 75 percent glass whereas sample 14141, the Cone Crater soil, contains less than 10 percent glass. In the < 62.5-micrometer fraction the glass fragments are generally highly angular and colorless to pale-green. With increasing grain size, dark-brown glass fragments, many of which appear to be agglutinates, are more abundant. Glass spheres are present but are not common. Several examples of compound glass spheres (one glass enclosing a second glass) were observed in samples 14148 and 14163.

The proportion of lithic fragments in the soils increases with grain size and reaches 70 to 100 percent in the 1- to 2-millimeter fraction. Lithic fragments include both fragmental and homogeneous crystalline rocks. The fragmental rock particles predominate over the crystalline rock particles and, in some

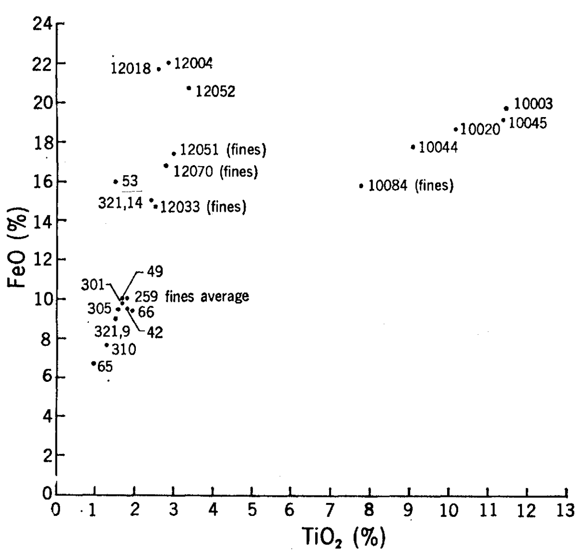

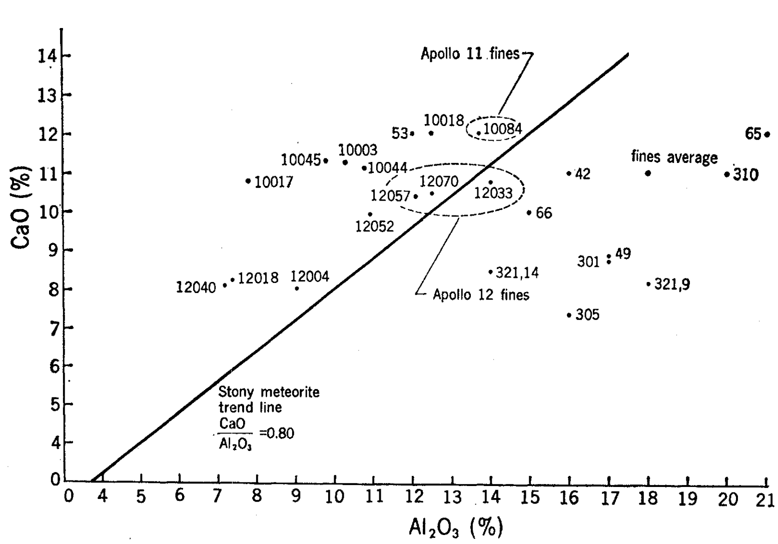

Fig. 9 (left). Contents of FeO as a function of the content of TiO_2 for selected lunar samples. Apollo 11 data are from a compilation by J. Warner (*13*); Apollo 12 data are from Compston *et al.* (*13*). Fig. 10 (right). Content of Al_2O_3 as a function of the content of CaO for selected lunar samples. Apollo 11 and Apollo 12 data are from the same sources as the data of Fig 9.

samples, crystalline rock fragments are absent. The lithic fragments are similar (in modal variability and range of types) to the lithic clasts found in the fragmental rocks described above. Fragments of crystalline rocks compose about 40 percent of the 1- to 2-millimeter fraction from the bottom of the trench, and most of them are plagioclase-rich (60 to 70 percent) with subophitic orthopyroxene. Clinopyroxene, opaque minerals (mostly ilmenite), and mesostasis are also present.

Mineral fragments are most abundant in the 37- to 62.5-micrometer fraction, consisting of angular grains of plagioclase, clinopyroxene, olivine, orthopyroxene, and opaque minerals in decreasing order of abundance. The ratios of plagioclase to clinopyroxene range from 16 : 1 to 1 : 2; the ratio varying not only from sample to sample but from one size fraction to another.

Sample 14141, the Cone Crater soil, is more coarse-grained (median grain size, about 0.74 millimeter), and its glass content is very low (less than 10 percent in the fraction larger than 0.5 millimeter). It contains a high content of fragmental rock fragments (40 to 60 percent), even in the finest size fractions (less than 62.5 micrometers). The remainder of the material is glass-bonded fragmental rock.

Cores

The astronauts on the Apollo 14 mission had more difficulty driving the core tubes than the crew of Apollo 12. These results indicate that the soil at this location is stronger with depth than had been previously supposed. Consequently, the Apollo 14 core tubes are poorer in terms of sample recovery and quality than those returned on the Apollo 12 mission.

Four cores, consisting of one double tube and two single tubes, were returned from the Fra Mauro site. None has been opened for study, but stereo x-radiographs have been taken to determine the amount of samples, texture, layering, and amount of disturbance of each core.

The double core (39.5 centimeters long, 209 grams) collected at station "A" during the traverse on EVA 2 shows textural changes which may represent at least seven and possibly nine layers, ranging in thickness from 1 to 13 centimeters. Overall, there is a pronounced decrease in grain size from the bottom to the top of the core. Near the base some 10 to 15 percent of the rock fragments are longer than 5 millimeters, whereas near the top there are only a few particles longer than 2 millimeters. The largest rock fragment visible in the x-radiographs is 1.2 centimeters long.

A single core (16.5 centimeters long, 81 grams) collected at Triplet Crater exhibits, on the basis of textural changes visible in the x-radiographs, at least three layers ranging from 0.5 to 5 centimeters thick. The soil appears to consist of 10 to 20 percent fragments longer than 2 millimeters in a matrix of fine sand or coarse silt. In this case, as in the double core, there is a crude grading of particles longer than 2 millimeters, from the base to the top of the core.

For another single core (12.5 centimeters long, 71 grams) collected at

Table 1. Elemental abundances; ppm, parts per miliion.

Component	Apollo 14 sample number											Fines average
	053	321,14	049	310	321,9	042	301	065	066	305	259	
Si (%)	22.6	22.4	22.9	23.5	23.5	24.0	22.9	22.6	24.0	23.0	22.6	22.5
Al (%)	6.4	7.4	9.0	10.6	9.5	8.5	9.0	11.1	8.0	8.5	9.5	9.3
Mg (%)	5.0	7.2	6.6	4.8	6.6	5.2	6.6	5.0	5.7	7.8	5.5	5.9
Fe (%)	12.6	10.1	7.6	6.0	7.0	7.4	7.6	5.3	7.3	7.4	7.8	8.0
Ca (%)	8.5	6.1	6.4	7.8	5.8	7.4	6.3	8.5	7.1	5.3	7.8	7.4
Ti (%)	0.9	1.4	1.0	0.8	0.9	1.1	1.0	0.6	1.1	1.0	1.1	1.1
Na (%)	.28	0.30	0.63	.47	.42	0.36	0.58	.68	0.42	0.63	0.38	0.42
K (%)	.12	.28	.44	.44	.46	.52	.60	.83	1.0	1.0	.42	.43
Mn (%)	.22	.20	.14	.11	.12	.12	.15	.09	0.12	0.14	.14	.15
Cr (%)	.30	.29	.13	.11	.11	.12	.12	.07	.09	.12	.14	.14
Ba (ppm)	190	380	670	630	730	820	920	820	960	930	570	638
Co (ppm)	48	33	40	31	32	56	44	19	39	32	39	44
Cu (ppm)	13	13	16	11	7	19	17	6	7	13	14	18
La (ppm)	10	40	63	36	65	70	92	32	72	54	46	49
Li (ppm)	11	18	20	19	19	19	20	20	25	23	18	21
Ni (ppm)	14	180	260	165	240	280	230	60	210	205	320	304
Nb (ppm)	19	22	52	43	46	68	63	57	60	49	40	48
Rb (ppm)	2	7	14	15	14	14	17	33	29	31	10	13
Sc (ppm)	90	43	25	20	16	30	31	16	24	22	21	24
Sr (ppm)	180	140	200	250	180	210	240	250	220	200	170	206
V (ppm)	135	85	48	35	32	74	63	46	52	52	50	51
Yb (ppm)	10	20	28	30	28	27	33	27	31	28	24	24
Y (ppm)	90	160	220	180	220	110	260	200	250	210	170	210
Zr (ppm)	310	670	880	930	860	1030	1000	980	970	900	720	922
SiO_2 (%)	48.	48.	49.	50.	50.	51.	49.	48.	51.	49.	48.	48.
Al_2O_3 (%)	12.	14.	17.	20.	18.	16.	17.	21.	15.	16.	18.	18.
MgO (%)	8.4	12.	11.	8.0	11.	8.6	11.	8.3	9.5	13.	9.2	9.9
FeO (%)	16.	13.	10.	7.7	9.0	9.5	9.8	6.8	9.4	9.5	10.	10.
CaO (%)	12.	8.5	8.9	11.	8.2	11.	8.8	12.	10.	7.4	11.	11.
TiO_2 (%)	1.5	2.4	1.7	1.3	1.5	1.8	1.7	0.95	1.9	1.6	1.8	1.8
Na_2O (%)	0.38	0.40	0.85	0.63	0.58	0.48	0.78	.92	0.58	0.85	0.52	0.57
K_2O (%)	.14	.33	.53	.53	.56	.63	.72	1.0	1.2	1.2	.50	.52
MnO (%)	.29	.26	.18	.14	.15	.16	.19	0.12	0.16	0.18	.18	.19
Cr_2O_3 (%)	.44	.42	.19	.16	.16	.18	.17	.10	.13	.18	.20	.20
ZrO_2 (%)	.04	.05	.07	.13	.12	.14	.07	.13	.13	.12	.10	.12
Total	99.2	99.4	99.5	99.5	99.4	99.5	99.3	99.3	99.0	99.1	99.5	100.3

Table 2. Gamma-ray analysis of lunar samples; dpm, disintegrations per minute; ppm, parts per million.

Sample number	Weight (g)	K (wt. %)	Th (ppm)	U (ppm)	^{26}Al (dpm/kg)	^{22}Na (dpm/kg)	^{56}Co (dpm/kg)	Remarks
				Clastic rocks				
14045	65	0.36 ± 0.04	13.8 ± 1.4	3.7 ± 0.5	130 ± 40	83 ± 25		
14066	510	.69 ± 0.07	15.3 ± 1.5	4.1 ± 0.6	110 ± 20	52 ± 10		
14082	63	.18 ± 0.02	4.6 ± 0.5	1.4 ± 0.2	140 ± 30	68 ± 14		White clasts
14301	1361	.55 ± 0.05	12.8 ± 1.3	3.6 ± 0.5	53 ± 11	36 ± 7		
14302	381	.55 ± 0.05	14.3 ± 1.4	3.8 ± 0.6	85 ± 17	52 ± 10		
14315	115	.30 ± 0.03	9.1 ± 0.9	2.5 ± 0.4	160 ± 30	60 ± 12		
14318	600	.49 ± 0.05	12.8 ± 1.3	3.3 ± 0.5	120 ± 20	36 ± 7		
				Crystalline rocks				
14053	251	.088 ± 0.009	2.24 ± 0.22	0.64 ± 0.10	98 ± 20	59 ± 12		
14310	3425	.49 ± 0.06	13.7 ± 1.7	3.7 ± 0.6	80 ± 20	55 ± 15	25 ± 5	Ge(Li) detector used
				< 1-mm fines				
14163	491	.48 ± 0.05	13.9 ± 1.4	3.9 ± 0.6	78 ± 16	45 ± 9		Bulk soil
14259	495	.42 ± 0.04	13.4 ± 1.3	3.8 ± 0.6	220 ± 40	84 ± 17		Comprehensive soil
14148	70	.41 ± 0.04	14.9 ± 1.5	4.1 ± 0.6	190 ± 40	70 ± 14		Top trench
14156	136	.40 ± 0.04	14.5 ± 1.4	3.9 ± 0.6	180 ± 40	66 ± 13		Middle trench
14149	85	.44 ± 0.4	14.8 ± 1.5	3.9 ± 0.6	150 ± 30	58 ± 12		Bottom trench

Triplet Crater about 15 percent of the rock fragments are longer than 2 millimeters in a fine-grained matrix. The sample has been loose in the tube and is highly disturbed.

Chemical Composition

Preliminary analyses of both major element and trace element concentrations of soil and rock samples were obtained by the following techniques: (i) emission spectrographic analysis, (ii) gamma-ray spectroscopy, and (iii) direct combustion of carbon to carbon dioxide for total carbon analysis by means of analytical methods similar to those described previously (*6*). The results of these analyses are summarized in Tables 1, 2, and 3. Some of the data shown there are also summarized in Figs. 8 and 9 where they are compared with analyses of other lunar samples. The comparisons given in Fig. 10 show that, with the exception of sample 14053, the Apollo 14 samples have consistently lower contents of iron oxide than mare basalts. Their iron content is, in fact, similar to that of most terrestrial basalts. In addition, it is seen (Fig. 11), again with the exception of sample 14053, that the Apollo 14 samples have consistently higher contents of aluminum oxide than mare basalts.

The concentrations of minor or trace elements such as potassium, rubidium, uranium, thorium, barium, yttrium, and niobium are much higher than those found for the mare basalts (Fig. 11). The concentrations of these elements are also similar to the values observed for the exotic fragments in the Apollo 12 soil.

Table 3. Total carbon abundances; ppm, parts per million.

Sample number	Carbon (ppm)	Remarks
	Soils	
14163	145 ± 10	Bulk soil, < 1 mm
14163	150 ± 10	Bulk soil, < 1 mm
14163	70 ± 10	Bulk soil, < 1 mm
14163	120 ± 10	Bulk soil, < 1 mm
14259	160 ± 10	Comprehensive soil, < 1 mm
14148	160 ± 10	Trench soil (top), < 1 mm
14156	180 ± 10	Trench soil (middle), < 1 mm
14149	135 ± 10	Trench soil (bottom), < 1 mm
14141	80 ± 10	Cone Crater soil, < 1 mm
	Fragmental rocks	
14042	225 ± 10	
14047	210 ± 10	
14049	190 ± 10	
14313	130 ± 10	
14066	90 ± 10	
14063	80 ± 10	
14301	50 ± 10	
14305	32 ± 8	
14321	28 ± 8	
	Crystalline rocks	
14310	35 ± 8	Fine-grained basaltic rock

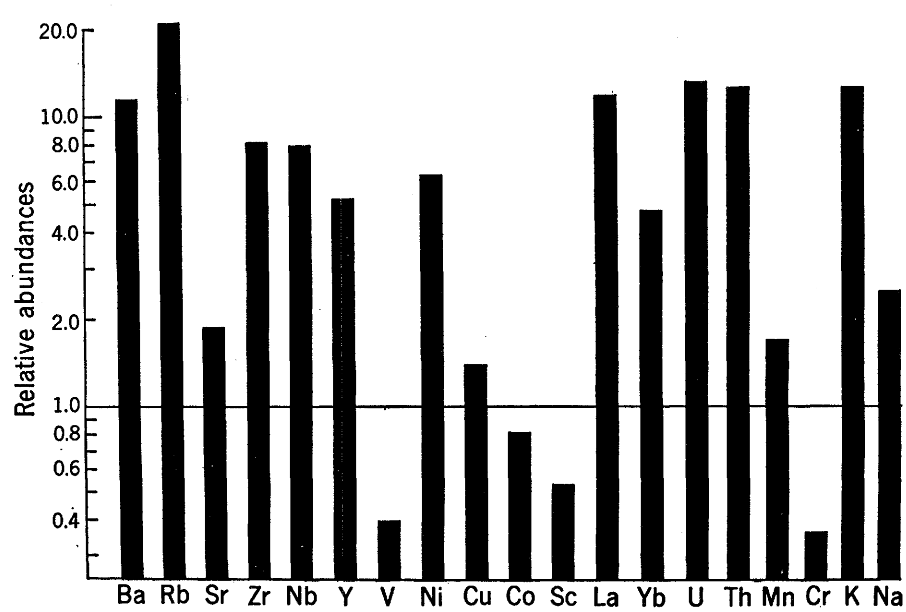

Fig. 11. Relative abundances of minor and trace elements in Apollo 14 rocks with respect to Apollo 12 rocks (normalized to unity).

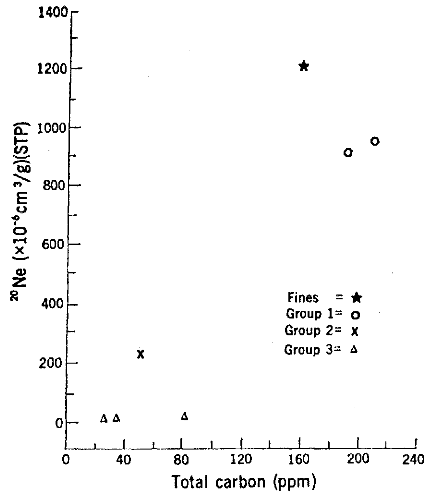

Fig. 12. Plot of ^{20}Ne derived from the solar wind as a function of the carbon content. Samples are classified according to their coherence. Note that the carbon values appear to follow the neon values and that there is some correlation with rock type. STP, standard temperature and pressure.

The average nickel content of fragmental rocks in the Apollo 11 samples is similar to that of the Apollo 11 soils, whereas the nickel content of the Apollo 14 fragmental rocks is significantly lower than that of the Apollo 14 soil.

Rock 14310 is very similar in composition to the fragmental rocks. The chemically most distinct sample analyzed is sample 14053 which mineralogically and chemically resembles more closely the basaltic rocks of Apollo 12 type than other rocks or soils from Fra Mauro base. The data presented here, although preliminary, clearly support the hypothesis put forth on the basis of the Apollo 12 soil samples, namely, that some premare lunar materials have been produced by extensive and efficient chemical differentiation processes.

Results of the analyses for total carbon are given in Table 3. The soil samples have total carbon contents ranging from 70 to 180 ppm, that is, within the range of total carbon found in the Apollo 11 and Apollo 12 samples. The trench samples do not show a significant variation in carbon content with depth.

The fine-grained fragmental rocks range in total carbon content from 28 to 225 ppm. The lowest carbon content was found in the largest rock (sample 14321), which has pronounced crystallinity. The fragmental rock samples analyzed may not be representative of the whole rocks because of the small size of the samples (200 milligrams), the heterogeneity of the rocks, and surface soil contamination. The only homogeneous crystalline rock (sample 14310) analyzed has a total carbon content of 35 ppm, a value similar to those of the basaltic rocks from Apollo 11 and Apollo 12.

In order to study the spallation effects of cosmic rays, ^{22}Na and ^{26}Al were analyzed in the same samples that were analyzed for potassium, thorium, and uranium. Techniques were the same as those reported previously (*6*). Results are listed in Table 2. These results are still preliminary, so that error limits are large; ^{54}Mn, ^{56}Co, and ^{46}Sc were detected in some samples.

In the soil the specific activity of ^{26}Al ranges from 78 disintegrations per minute per kilogram in the bulk fines to 221 disintegrations per minute per kilogram (soil from a range of depths up to at least 10 centimeters) in the comprehensive fines (soil from the top centimeter of the lunar surface). The specific activity of ^{22}Na ranges from 45 disintegrations per minute per kilogram (bulk fines) to 84 disintegrations per minute per kilogram (comprehensive fines).

In the rocks the specific activity of ^{26}Al ranges from 53 ± 11 disintegrations per minute per kilogram in rock 14301, which was almost buried in the lunar regolith, to 157 ± 31 disintegrations per minute per kilogram in rock 14315. The specific activity of ^{22}Na ranges from 36 ± 7 disintegrations per minute per kilogram (rocks 14318 and 14301) to 83 ± 25 disintegrations per minute per kilogram (rock 14045).

Orientation Based on the 25 January 1971 Solar Flare

A solar flare occurred on 25 January 1971, which permitted a unique opportunity to study radioactive products in lunar rocks induced by solar flares and allows the recent (since 24 January) surface orientation of certain rocks to be determined. Solar-flare protons produce ^{56}Co (half-life, 77 days) by (p,n) reaction on iron. The ^{56}Co is predominantly produced on the side of the rock facing the sun. The "top" and "bottom" of rock 14310 were determined by scanning the surface by means of a lithium-drifted germanium detector (40 cubic centimeters) for the emitted γ radiation of ^{56}Co.

Table 4. Total noble gas contents. Mass spectrometer sensitivity variations throughout the period of these analyses did not exceed ± 10 percent. However, since krypton was split between two gas fractions, the uncertainty in its abundance is ± 20 percent. Isotopic ratios and abundances have been corrected for blanks and multiplier discrimination. All extraction blanks were less than 15 percent with the exception of those abundances marked with an asterisk. Isotopic ratios of those samples with high gas concentrations are believed to be accurate to better than ± 2 percent. Isotopic ratios for those samples with low gas concentrations, and especially those to which large blank corrections were applied, are less accurate. In particular, the neon isotopic composition of sample 14063 (fragments) is not precisely determined because of large blank corrections. STP, standard temperature and pressure.

Sample number	Weight (mg)	Content [× 10^{-6} cm^3/g (STP)]				Content [× 10^{-9} cm^3/g (STP)]		$^{20}Ne/^{22}Ne$	$^{22}Ne/^{21}Ne$	$^{36}Ar/^{38}Ar$	$^{40}Ar/^{36}Ar$
		^{3}He	^{4}He	^{22}Ne	^{36}Ar	^{84}Kr	^{132}Xe				
14063,5 (fragments)	3.21	0.37	1,770	0.54*	2.31	6.8	3.2	15	14.6	5.21	99.2
14063,5 (whole rock)	17.08	0.50	1,980	1.40	2.31	0.80	0.19*	12.8	22.9	5.24	61.8
14066,2	12.86	0.19	2,020	0.22*	0.52	0.87	0.39	11.5	8.77	4.64	382
14305,9	30.18	0.168	2,510	0.062*	0.060*	0.23*	0.14*	6.96	2.40	2.28	2,205
14321,13	27.40	0.204	1,313	0.189*	0.41*	0.56*	0.28*	10.7	5.80	4.15	260
14301,7	1.89	4.49	12,300	18.6	38.0			12.0	29.5	4.94	16.2
14301,7	18.65				22.3	9.7	2.9			5.18	14.9
14047,2	1.80	23.1	54,400	73.4	283			13.0	26.6	5.25	1.38
14047,2	17.0				216	144	23			5.27	1.37
14049,3	1.77	20.0	47,600	71.6	252			12.6	25.0	5.24	1.90
14049,3	15.7				188	119	21			5.28	1.81
14259,10	1.55	36.8	77,700	95.4	328			12.7	27.7	5.28	1.37
14259,10	17.12				202	348	92			5.31	1.25

Noble Gases

The abundances and isotopic compositions of the five stable noble gases were determined by mass spectrometry in one soil sample and in seven fragmental rocks (Table 4). The concentrations of noble gases in soil sample 14259 and in rocks 14047, 14059, and 14301 are approximately two orders of magnitude higher than in the other four rocks measured. These gases are predominantly of a solar wind–implantation origin and occur in concentrations similar to those measured in soil and breccia returned on the two previous Apollo missions. Elemental abundance ratios and the isotopic ratios of helium, neon, and argon for these four samples are also similar to those of solar wind–implanted gases from earlier Apollo samples.

Rocks 14063, 14066, 14305, and 14321 exhibit noble gases resulting from radiogenic decay (^{40}Ar and ^{4}He) and cosmic-ray interactions, as well as small, variable amounts of solar wind gases which probably occur in contaminating lunar dust on the surfaces of the small (average weight, 13 milligrams) samples. Combining the radiogenic ^{40}Ar concentrations in these rocks with the potassium contents (Tables 1 and 2) yields gas retention ages ranging from 2.8×10^9 to 3.8×10^9 years. Sample heterogeneity and possible gas loss make these values uncertain, and, at best, they represent only lower limits to the crystallization ages of these rocks. However, unlike the fragmental rocks of Apollo 11 and Apollo 12, these samples should yield accurate ages by the $^{40}Ar/^{39}Ar$ method. If the formation of fragmental rocks with a low content of solar wind gas involved the incorporation and degassing of surface fine material, this formation must have occurred prior to 3×10^9 years ago in order for radiogenic ^{40}Ar to accumulate. Alternatively, material incorporated into these four rocks never contained a significant component of solar wind.

Calculated concentrations of some spallation-produced noble gas isotopes in these samples are listed in Table 5. Also listed are some approximate surface exposure ages calculated from these spallation isotopes. Rocks 14063, 14066, 14321, and 14305 all show similar concentrations of each spallation nuclide. Exposure ages generally fall in the range from 10×10^6 to 20×10^6 years, with reasonable agreement among the ages based on different spallation isotopes. These four rocks may actually have had the same exposure time, with the age variations resulting from differing shielding and analytical uncertainties. One could speculate that these rocks date the time of a single cratering event, possibly Cone Crater. These ages are considerably lower than typical ages of 40×10^6 to 500×10^6 years for rocks returned by the Apollo 11 and Apollo 12 missions. Rock samples 14047 and 14049 and soil sample 14259 exhibit spallation concentrations approximately an order of magnitude greater than those of rocks 14063, 14066, 14321, and 14305; but because of the presence of solar wind gases, these abundances are highly uncertain.

Table 5. Cosmic-ray, spallation-produced noble gases and exposure ages. Concentrations of spallation isotopes have been calculated from the data in Table 1. Ages have been calculated on the basis of chemical data from Tables 1 and 2 and production rates given by Bogard *et al.* (*12*).

Sample number	Content [$\times 10^{-8}$ cm^3/g (STP)]				Age ($\times 10^6$ years)		
	^{3}He	^{21}Ne	^{38}Ar	^{128}Xe	^{21}Ne	^{38}Ar	^{128}Xe
14063,5		1.6	1.0	0.001	10	9	
14063,5 (fragments)	< 37	2.0	1.3	0.003	13	10	
14066,2	< 19	1.9	1.7	0.002	11	14	9
14321,13	< 20	2.7	2.5	0.0017	16	24	22
14305,9	< 17	2.5	1.7	0.0021	14	19	11
14047,2		~ 33					
14049,3		~ 50					
14259,10		~ 26				~ 170	

The isotopic compositions of krypton and xenon measured in several of the samples are presented in Table 6. In samples 14259, 14049, 14047, and 14301 the relative isotopic abundances are similar to those of Apollo 11 and Apollo 12 samples for which solar wind gases were determined with the addition of a spallation component. For these samples we subtracted a solar wind component identical to that deduced by Eberhardt *et al.* (*8*) from Apollo 11 soils. The resulting spallation isotope spectra are generally similar to those determined for earlier lunar rocks. Xenon-131 exhibits a high relative yield as in earlier lunar samples, and, for sample 14259, the ^{129}Xe and ^{132}Xe yields are also enhanced. Although the uncertainties in these spectra are large, there appear to be definite differences in the various spallation krypton and xenon spectra. Spallation spectra are even more uncertain for the rocks with a low amount of gas because of the necessary corrections for fission-produced and atmospheric xenon, and only one such rock (rock 14321) is listed in Table 6. Rock 14301,7 shows large concentrations of the fission-produced isotopes ^{134}Xe and ^{136}Xe (1.5×10^{-10} cubic centimeter of excess ^{136}Xe per gram). If our sample has the characteristic measured uranium concentration of 3.5 ppm (Table 2), this amount of excess ^{136}Xe is considerably more than the amount that could be produced by the spontaneous fission of ^{238}U in 4.5×10^9 years. However, with the possible exception of sample 14301, there appears to be no need to invoke extinct radionuclides to explain the observed abundances of ^{129}Xe and ^{136}Xe.

Biology

No viable organism has been found in the lunar material and there is no evidence of fossil material. Direct observations involved light microscopy with white light, ultraviolet light, and phase-contrast techniques. A wide variety of biological systems are now being tested with lunar material to determine if there is any toxicity, microbial replication, or pathogenicity. Histological studies are being made to determine whether or not there is any evidence of pathogenicity. Other activities involve extensive in vitro study of the lunar samples.

Summary

The major findings of the preliminary examination of the lunar samples are as follows:

1) The samples from Fra Mauro base may be contrasted with those from Tranquillity base and the Ocean of Storms in that about half the Apollo 11 samples consist of basaltic rocks, and all but three Apollo 12 rocks are basaltic, whereas in the Apollo 14 samples only two rocks of the 33 rocks over 50 grams have basaltic textures. The samples from Fra Mauro base consist largely of fragmental rocks con-

Table 6. Measured krypton and xenon ratios. All values have been discrimination-corrected. Uncertainties given are statistical fluctuations of 1 standard deviation.

Sample number	$^{i}Kr/^{84}Kr$					$^{i}Xe/^{132}Xe$							
	78	80	82	83	86	124	126	128	129	130	131	134	136
14259,10	0.0089 ± 0.0005	0.0466 ± 0.0007	0.2097 ± 0.0011	0.2092 ± 0.0018	0.3025 ± 0.0015	0.0121 ± 0.0004	0.0179 ± 0.0005	0.1063 ± 0.0012	1.091 ± 0.007	0.1770 ± 0.0018	0.8808 ± 0.0043	0.3655 ± 0.0019	0.2941 ± 0.0015
14047,2	0.028 ± 0.001	0.0464 ± 0.003	0.2105 ± 0.0011	0.2113 ± 0.0020	0.3039 ± 0.0016	0.0127 ± 0.0012	0.0230 ± 0.0004	0.1121 ± 0.0010	1.071 ± 0.011	0.1809 ± 0.0012	0.9041 ± 0.0056	0.3642 ± 0.0025	0.2945 ± 0.0018
14049,3	0.0113 ± 0.0001	0.0511 ± 0.0004	0.2167 ± 0.0010	0.2204 ± 0.0014	0.3043 ± 0.0029	0.0181 ± 0.0003	0.0291 ± 0.0004	0.1216 ± 0.001	1.075 ± 0.007	0.1866 ± 0.0015	0.9251 ± 0.0044	0.3641 ± 0.0019	0.2949 ± 0.0017
14301,7	0.055 ± 0.005	0.1959 ± 0.0041	0.2133 ± 0.0021	0.2072 ± 0.0063	0.3004 ± 0.0021	0.0133 ± 0.0016	0.0216 ± 0.0013	0.1059 ± 0.0051	1.058 ± 0.008	0.1697 ± 0.0038	0.8824 ± 0.0063	0.4048 ± 0.0031	0.3447 ± 0.0050
14321,13	0.084 ± 0.013	0.086 ± 0.011	0.252 ± 0.009	0.259 ± 0.008	0.301 ± 0.008	0.031 ± 0.010	0.051 ± 0.009	0.163 ± 0.017	1.102 ± 0.031	0.206 ± 0.016	0.945 ± 0.021	0.389 ± 0.011	0.325 ± 0.012

taining clasts of diverse lithologies and histories. Generally the rocks differ modally from earlier lunar samples in that they contain more plagioclase and contain orthopyroxene.

2) The Apollo 14 samples differ chemically from earlier lunar rocks and from their closest meteorite and terrestrial analogs. The lunar material closest in composition is the KREEP component (potassium, rare earth elements, phosphorus), "norite," "mottled gray fragments" (*9*) from the soil samples (in particular, sample 12033) from the Apollo 12 site, and the dark portion of rock 12013 (*10*). The Apollo 14 material is richer in titanium, iron, magnesium, and silicon than the Surveyor 7 material, the only lunar highlands material directly analyzed (*11*). The rocks also differ from the mare basalts, having much lower contents of iron, titanium, manganese, chromium, and scandium and higher contents of silicon, aluminum, zirconium, potassium, uranium, thorium, barium, rubidium, sodium, niobium, lithium, and lanthanum. The ratios of potassium to uranium are lower than those of terrestrial rocks and similar to those of earlier lunar samples.

3) The chemical composition of the soil closely resembles that of the fragmental rocks and the large basaltic rock (sample 14310) except that some elements (potassium, lanthanum, ytterbium, and barium) may be somewhat depleted in the soil with respect to the average rock composition.

4) Rocks display characteristic surface features of lunar material (impact microcraters, rounding) and shock effects similar to those observed in rocks and soil from the Apollo 11 and Apollo 12 missions. The rocks show no evidence of exposure to water, and their content of metallic iron suggests that they, like the Apollo 11 and Apollo 12 material, were formed and have remained in an environment with low oxygen activity.

5) The concentration of solar wind–implanted material in the soil is large, as was the case for Apollo 11 and Apollo 12 soil. However, unlike previous fragmental rocks, Apollo 14 fragmental rocks possess solar wind contents ranging from approximately that of the soil to essentially zero, with most rocks investigated falling toward one extreme of this range. A positive correlation appears to exist between the solar wind components, carbon, and ^{20}Ne, of fragmental rocks and their friability (Fig. 12).

6) Carbon contents lie within the range of carbon contents for Apollo 11 and Apollo 12 samples.

7) Four fragmental rocks show surface exposure times (10×10^6 to 20×10^6 years) about an order of magnitude less than typical exposure times of Apollo 11 and Apollo 12 rocks.

8) A much broader range of soil mechanics properties was encountered at the Apollo 14 site than has been observed at the Apollo 11, Apollo 12, and Surveyor landing sites. At different points along the traverses of the Apollo 14 mission, lesser cohesion, coarser grain size, and greater resistance to penetration was found than at the Apollo 11 and Apollo 12 sites. These variations are indicative of a very complex, heterogeneous deposit. The soils are more poorly sorted, but the range of grain size is similar to those of the Apollo 11 and Apollo 12 soils.

9) No evidence of biological material has been found in the samples to date.

Discussion

The compositions of the Apollo 14 rocks are compatible with their derivation as an ejecta deposit from the Mare Imbrium basin. These rock samples are largely fragmental and show pronounced shock effects, and the composition of most samples is distinctly different from that of basaltic rocks from lunar maria. The crystallinity observed in many of the fragmental rocks is compatible with a single very large impact event in which annealing took place within a thick, hot ejecta blanket.

Fragmental rocks within fragmental rocks and the apparently complex histories of nearly all rocks deserve serious study. A number of possible explanations and their combinations may be offered: (i) excavation by the Imbrian event of preexisting brecciated material including ejecta from the earlier Serenitatis cratering event; (ii) formation of breccia within breccia during the Imbrian event; and (iii) local cratering events superimposed on the Imbrian event.

If the rocks were excavated by the Imbrian event, they represent a sample of the premare lunar surface to a depth of some tens of kilometers. The presence of microscopically visible exsolution in pyroxenes indicates that some of the rocks from which the fragmental rocks were derived cooled more slowly and thus presumably crystallized at greater depths than mare basalts which typically exhibit only submicroscopic pyroxene exsolution. The range of compositions and textures of clasts within the fragmental rocks suggests that their source area had a complex history. Nevertheless, the major and trace element abundances of the fragmental rocks are so similar to those of the soils that extensive mixing must have occurred, and we can infer that the bulk composition of the source area was enriched in elements such as barium, strontium, rubidium, and potassium and depleted in iron with respect to mare basalts. The mineralogical and chemical similarity between the Fra Mauro material, fragments with a high abundance of KREEP component or "norite," and the dark portion of rock 12013 from the Apollo 12 mission suggests that material of this composition is widespread on the lunar surface. Since this material is even further removed in composition from average solar or chondritic abundances than the mare basalts, a history of profound premare lunar differentiation which produced a lunar crust is indicated. This differentiation could have occurred during the accretion of the moon with the accumulation of material rich in incompatible elements near the surface, or in a process of crust formation involving the fractionation of a considerable volume of the moon early in lunar history.

The basaltic rocks from the mare regions cannot be derived by partial melting of material of Fra Mauro composition, and the reverse is also true. Therefore, it would appear that neither the mare nor the nonmare areas of the moon are representative of the bulk composition of the moon, but both mare and nonmare areas may represent partial melting products of the lunar interior. The extent and variability of the rocks formed in the early lunar crust cannot be determined without samples from other uplands areas; there is no compelling reason yet to assume that Fra Mauro–like material is representative of the lunar highlands.

References and Notes

1. The people who contributed directly to obtaining the data and to the preparation of this article are: D. H. Anderson, Manned Spacecraft Center (MSC); M. N. Bass, MSC; A. D. Bennett, Brown and Root-Northrup (BRN); D. D. Bogard, MSC; R. Brett, MSC; L. G. Bromwell, Massachusetts Institute of Technology (M.I.T.); P. Butler, Jr., MSC; W. D. Carrier III, MSC; R. S. Clark, MSC; T. Cobleigh, Linnaean Society, Widdicombe; M. B. Duke, MSC; P. W. Gast, MSC; E. K. Gibson, Jr., MSC; W. R. Hart, BRN; G. H. Heiken, MSC; W. C. Hirsch, BRN; F. Hörz, MSC; E. D. Jackson, U.S. Geological Survey (USGS); P. H. Johnson, BRN; J. E. Keith, MSC; C. F. Lewis, Arizona State University (ASU); John F. Lindsay, MSC; J. R. Martin, BRN; W. C. Melson, U.S. National Museum; E. D. Mitchell, MSC; C. B. Moore, ASU; D. A. Morrison, MSC; W. B. Nance, BRN; W. C. Phinney, MSC; A. M. Reid, MSC; M. A. Reynolds, MSC; K. A. Richardson, MSC; W. I. Ridley, MSC; E. Schonfeld, MSC; A. B. Shepard, MSC; R. L. Sutton, USGS; N. J. Trask, USGS; J. Warner, MSC; R. B. Wilkin, BRN; H. G. Wilshire, USGS; D. R. Wones, M.I.T.
2. G. K. Gilbert, *Bull. Phil. Soc. Wash.* **12**, 241 (1893).
3. R. E. Eggleton, "Astrogeological Studies: Annual Progress Report, August 1962–July 1963," part A 6 (U.S. Geological Survey open-file report, Washington, D.C., 1963), pp. 46–63.
4. G. A. Swann, N. J. Trask, M. H. Hait, R. L. Sutton, *Science* **173**, 716 (1971).
5. "Apollo 14 Preliminary Science Report" (National Aeronautics and Space Administration, Washington, D.C., in press).
6. Lunar Sample Preliminary Examination Team, *Science* **165**, 1211 (1969); *ibid.* **167**, 1325 (1970).
7. D. E. Gault, W. L. Quaide, V. R. Oberbeck, in *Shock Metamorphism of Natural Materials*, B. French and N. M. Short, Eds. (Mono, Baltimore, 1968), p. 87.
8. P. Eberhardt, J. Geiss, H. Graf, N. Groegler, U. Kraehenbuehl, H. Schwaller, J. Schwarzmueller, A. Stettler, in *Proceedings of the Apollo 11 Lunar Science Conference*, A. A. Levinson, Ed. (Pergamon, New York, 1970), vol. 2, pp. 1037–1070.
9. A. T. Anderson, Jr., R. C. Newton, J. V. Smith, paper presented at the Proceedings of the Second Lunar Science Conference, Houston, January 1971; N. J. Hubbard, C. Meyer, Jr., P. W. Gast, H. Wiesmann, *Earth Planet. Sci. Lett.* **10**, 341 (1971); E. A. King, J. C. Butler, M. F. Carman, paper presented at the Proceedings of the Second Lunar Science Conference, Houston, January 1971; D. S. McKay, D. Morrison, J. Lindsay, G. Ladle, *ibid.*; C. Meyer, Jr., F. K. Aitken, P. R. Brett, D. S. McKay, D. A. Morrison, *ibid.*; W. Quaide, K. V. Oberbeck, T. Bunch, G. Polkowski, *ibid.*; J. A. Wood, U. Marvin, J. B. Reid, G. J. Taylor, J. F. Bowen, B. N. Powell, J. S. Dickey, Jr., *ibid.*
10. M. J. Drake, I. S. McCallum, G. A. McKay, D. F. Weill, *Earth Planet. Sci. Lett.* **9**, 103 (1970).
11. A. L. Turkevich, paper presented at the Proceedings of the Second Lunar Science Conference, Houston, January 1971.
12. D. D. Bogard, J. D. Funkhouser, O. A. Schaeffer, J. Zähringer, *J. Geophys. Res.* **76**, 2757 (1971).
13. J. Warner, unpublished continuing compilation, MSC Curator's Office; W. Compston, H. Berry, M. J. Vernon, B. W. Chappell, M. J. McKay, paper presented at the Proceedings of the Second Lunar Science Conference, Houston, January 1971.

14. The members of the Lunar Sample Preliminary Examination Team acknowledge the technical assistance of the following members of the NASA Manned Spacecraft Center, Brown and Root-Northrup, and Lockheed Electronics Corp. staffs; T. J. Allen, J. O. Annextad, R. Bell, L. Bennett, M. C. Brabham, E. P. Carranza, L. E. Cornitius, C. Cucksee, J. B. Dorsey, A. Eaton, P. Gilmore, P. Graf, G. M. Greene, D. W. Hutchinson, R. W. Irvin, D. Jezek, S. W. Johnson, C. E. Lee, E. A. Locke, D. Mann, T. M. McPherson, M. Mitchell, D. R. Moore, J. L. Nix, W. A. Parkan, D. S. Pettus, C. M. Polo, W. R. Partenier, G. R. Primeaux, J. Ramsay, S. Richards, M. K. Robbins, J. Schartzback, Jr., J. Siggin, L. A. Simms, K. L. Suit, N. Trent, N. L. Turner, L. Tyler, and D. R. White.